RECENT ADVANCES IN COMPUTATIONAL MODELING OF CONTINUOUS CASTING OF STEEL

Brian G. Thomas

Wilkins Professor of Mechanical & Industrial Engineering
University of Illinois, 1206 W. Green St., Urbana, IL 61801
217-333-6919; bgthomas@uiuc.edu

As computer power increases, computational models are able to contribute more to the understanding and design of complex processes such as the continuous casting of steel. Fluid flow models can now include phenomena such as transient behavior during steady casting, including particle transport, capture and removal. Heat flow models can include interfacial slag layer heat, mass and momentum balances, and nonequilibrium crystallization behavior, and can predict slag structure and friction with the mold. Stress models can be used to make quantitative predictions such as ideal mold taper and maximum casting speed to avoid problems such as off-corner longitudinal cracks. This paper shows recent examples of these models, and their comparison with experimental measurements. With increased effort to improve software capabilities, future models could serve as even more practical tools for design and trouble-shooting.

Introduction

Understanding and controlling the continuous casting process is important because it may introduce defects that persist into the final product, even after many later processing steps. These defects include oxide inclusions, porosity, segregation, and cracks. In addition to expensive plant experiments and water models, advanced computational models are increasingly able to generate this understanding. Helped by recent improvements in computer power and software, computational models can simulate phenomena ranging from metallurgical thermodynamics to fluid flow, heat transfer, solidification and stress generation. This paper shows recent examples of some these, based on recent work at the University of Illinois Continuous Casting Consortium.

Simulations of Fluid Flow in Nozzle and Mold

Turbulent Flow Model

Three-dimensional turbulent flow is being predicted in both the nozzle and mold using the Large Eddy Simulation code, UIFLOW [1]. This approach is more accurate than the standard K-ε turbulence model for transient flows [2], and not as computationally intensive as DNS (direct numerical simulation). An example for a trifurcated nozzle submerged 127mm deep into an 984mm wide x 132 mm thick stainless-steel caster is shown in Figure 1 (model domain) and Figure 2 (typical result) [3]. The velocities compare well with quantitative velocity measurements in a water model of this caster [4]. More importantly, the contour of the top surface, including level fluctuations can be modeled.

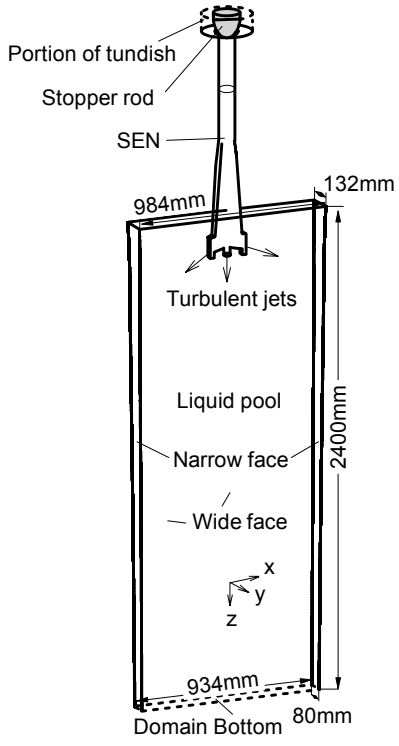

Figure 1. Computational domain of tri-furcated nozzle and thin-slab casting mold

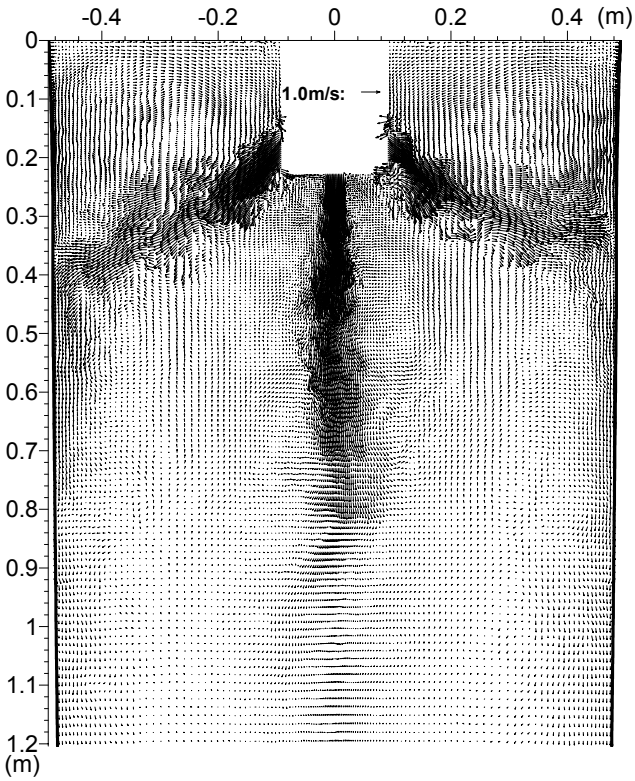

Figure 2. Typical instantaneous velocity vector plot at the center plane between wide faces

As shown in Figure 3, the model is able to simulate the top surface contour in both water model (measured from video frames) and in the actual steel caster (measured by inserting a steel sheet into the mold [5]). The shape follows expectations for a typical double-roll flow pattern. The jets impinging the narrow face wall turn upwards and downwards along the narrow face. The momentum of the upward jet lifts the meniscus by a height that can be approximated with a simple energy balance based on the pressure difference at the meniscus [4]. The surface contour is similar to that of the water model, except that the slag layer buoyancy increases the magnitude of the variations.

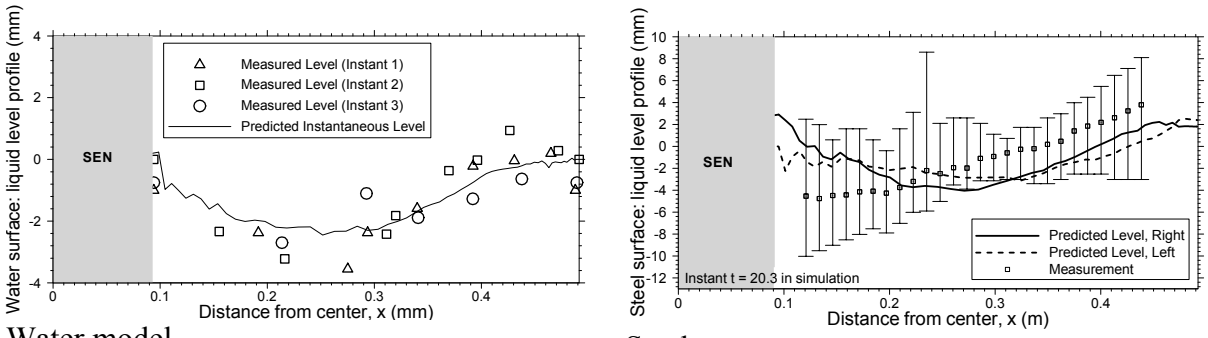

Water model Steel caster

Figure 3. Comparison of predicted and measured top surface liquid levels

Particle Motion and Entrapment

The flow pattern in the mold controls many phenomena that have a great effect on steel quality. One of these is the motion of inclusion particles, which can either be entrapped into the solidifying shell to form slivers and cracks, or can be safely removed into the top surface slag layer. Particle transport and capture in the continuous caster were simulated using a Lagrangian trajectory-tracking approach, based on the time-dependent flow fields just discussed [6]. The approach was first validated by a successful comparison of transport in a water model where over 50% of the 15,000 particles floated out in 100s. In the actual thin-slab caster, only about 8% of the 40,000 small particles were removed to the top surface [4].

Figure 4 shows a snapshot of the distribution of moving particles in the liquid pool. After a 9s sudden burst of particles entering the steel caster, about 4 minutes were needed for all of them to be captured or removed. Note that the particles move with an asymmetrical distribution, in spite of the symmetrical boundary conditions. This is caused by transients in fluid turbulence in the lower recirculation region, rather than by inlet variations at the nozzle port.

The computational results were further processed to predict the ultimate distribution of impurity particles in the solid thin slab after a short burst of inclusions entered the mold [4]. Figure 5 shows that most of the particles end up between 1m below and 1m above the location of the meniscus when they entered the mold. Note that the asymmetric particle distribution during the flow only leads to slight asymmetries in the distribution in the final product. The results were reprocessed to reveal the distribution of total oxygen content for a steady inclusion supply from the nozzle. Figure 6 shows how steel that initially contains 10ppm at the nozzle ports will ultimately range from only 6ppm in the interior to over 50ppm in spots near the narrow face. The greatest inclusion concentration is found near the surface, especially near the narrow faces. Further details are given elsewhere [3, 6]

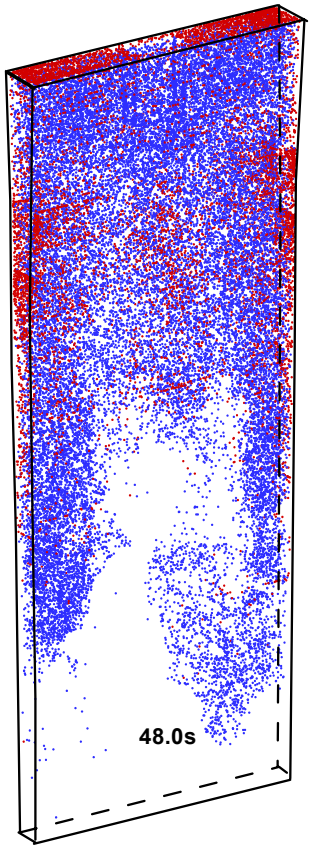

Figure 4. Distribution of moving particles, 48s after injection

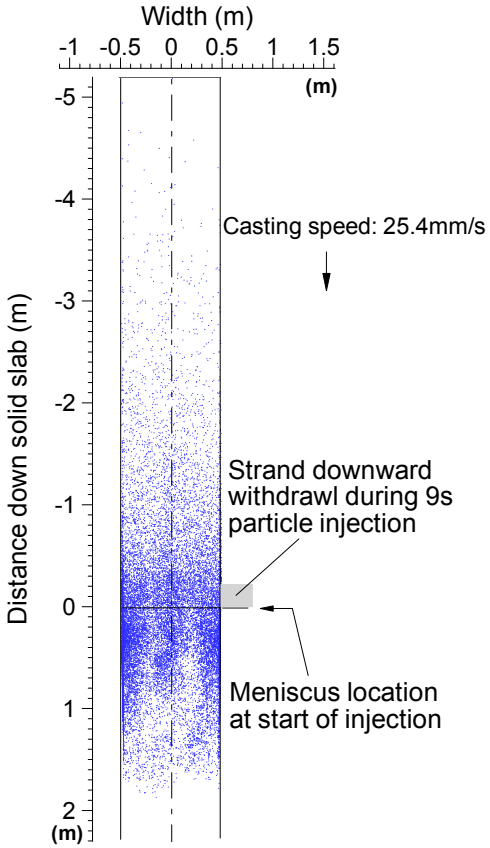

Figure 5. Final entrapment locations for a 9s-burst of particles: view from wide face

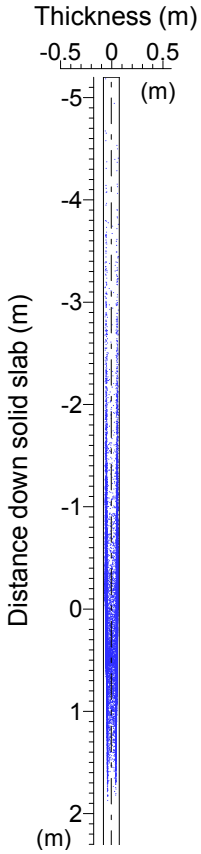

View from narrow face

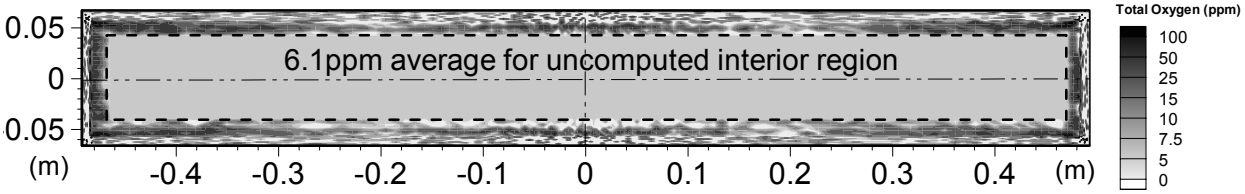

Figure 6. Predicted total oxygen concentration averaged along the slab length

The results of this work confirm the important role of flow transients in the transport and capture of particles during continuous casting, and can serve as a benchmark for future simplified models.

Modeling the Mold / Strand Interface

Heat transfer and solidification models are useful for many purposes, including the design of cooling water slots, shell thickness, and taper in the mold, finding the metallurgical length, the design of spray-cooling, and trouble-shooting the location of internal defects (hot tears that form at the solidification front). To study these phenomena, a model (CON1D) has been developed that includes a 1-D transient solidification model in the shell coupled with a 2-D steady model of the model [7]. It features a detailed treatment of the interface between the solidifying strand and the water-cooled mold which governs heat transfer in the process. To investigate mold flux behavior in the gap, the model includes a momentum balance on the solid and liquid flux layers in the gap, and a vertical-direction force balance between friction

against the mold wall and shell, and axial stresses in each slice through the solid flux layer (Figure 7). During each oscillation cycle, the model shows (in Figure 8) that the velocity profile in the liquid flux layer varies from the casting speed on the shell side (right) to the mold speed on the solid side attached to the mold wall (left), with a curved profile according the temperature-dependent viscosity of the liquid flux [8]. The accuracy of this part of the model is shown by its matching of results from a finite difference model of flow in the gap.

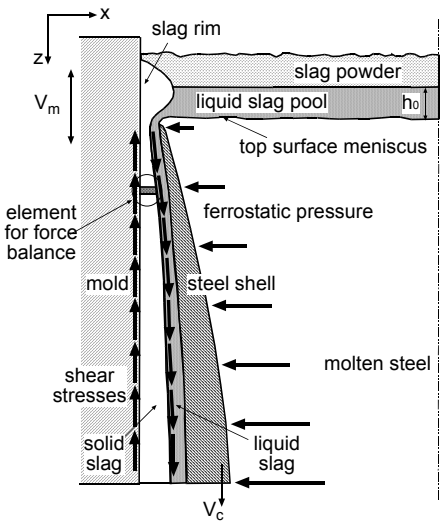

Figure 7 -Schematic of interfacial gap phenomena in continuous casting mold

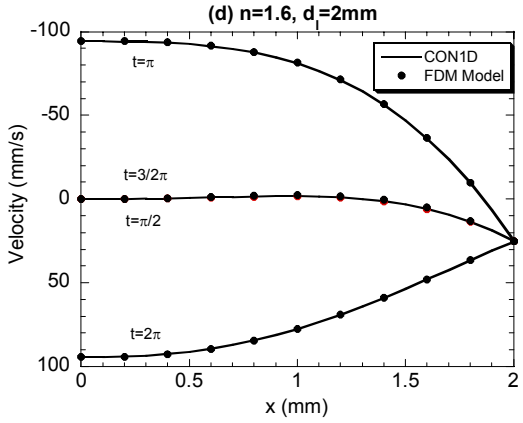

Figure 8 -Velocity profiles in liquid flux layer (for viscosity exponent = 1.6 and film thickness = 2mm)

The properties of mold flux change greatly when the flux crystallizes, which depends strongly on the thermal history [9]. Figure 9 compares the cooling curves computed at different positions across the thickness of the interfacial gap layers, during continuous casting with two different mold flux compositions. Details on the slag properties and casting conditions are given elsewhere [8]. The left frames show the temperature profiles along the length of the mold, while the right frames replot the data against time, so it can be compared with TTT diagrams measured for these two fluxes. The flux carried in the oscillation marks accounts for a significant fraction of the total flux consumed. It stays quite hot (exiting the mold around 1100 ^{o}C), and moves at the casting speed, so stays in the mold only for a short time in the mold (right). The flux near the mold wall cools to very low temperatures (left), and moves much more slowly, staying in the mold for over an hour (right). The cooling curves for most of slag A cross the transformation line for this composition, forming a crystalline layer except for the 0.2mm closest to the mold wall. Slag G, however, is seen to cool below the nose of the TTT curve, indicating that it will remain glassy.

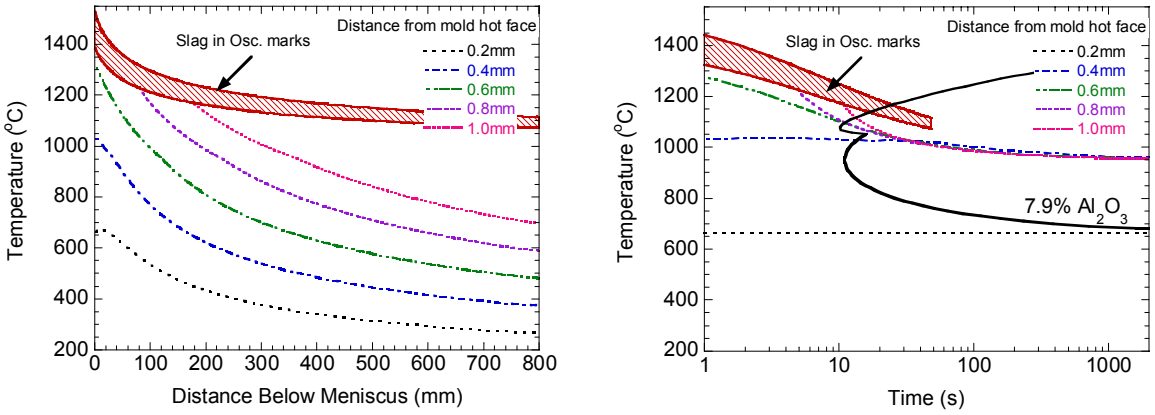

(a) Slag A (Crystalline)

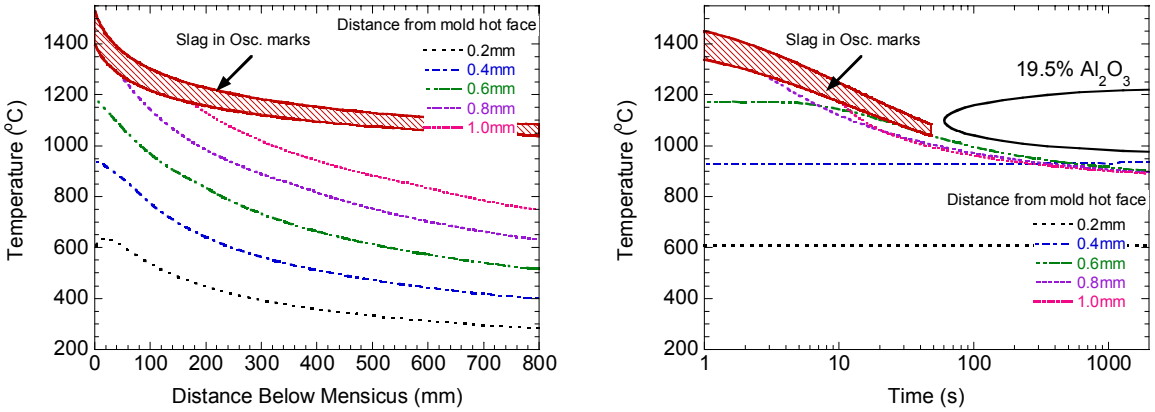

(b) Slag G (Glassy)

Figure 9 -Slag layer cooling history with attached slag and measured TTT curves

Friction Predictions

The model predicts that friction force depends mainly on whether the steel surface temperature falls below the solidification temperature of the flux. High in the mold, the flux against the steel shell is molten, so shear stress (friction) against the mold wall is very low (Figure 10). Low in the mold, the flux layer has become completely solid, is consumed by slow movement of the solid layer against the mold. This creates high friction forces, which alternate between upward and downward at different times during the oscillation cycle. The total friction force is obtained by integrating the shear stress profile over the mold surface, and can be measured in the plant using accelerometers.

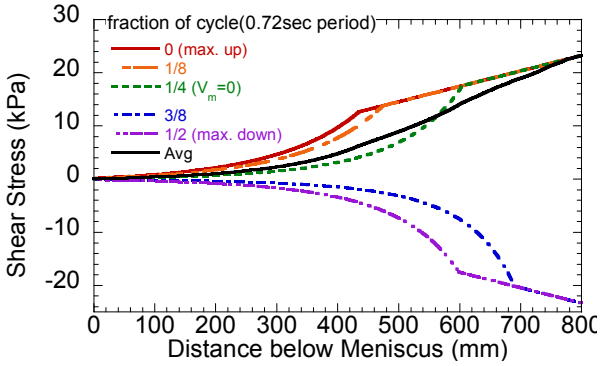

Figure 10 -Shear stress down the mold wall with "moving" solid layer (Slag A)

Figure 11 compares the friction forces obtained for three different scenarios. An attached solid layer involves liquid lubrication over the entire mold length, which produces very low friction forces that can also be distinguished by a smooth sinusoidal variation with time. Complete solidification of the flux in the gap, and the accompanying moving solid layer, produces

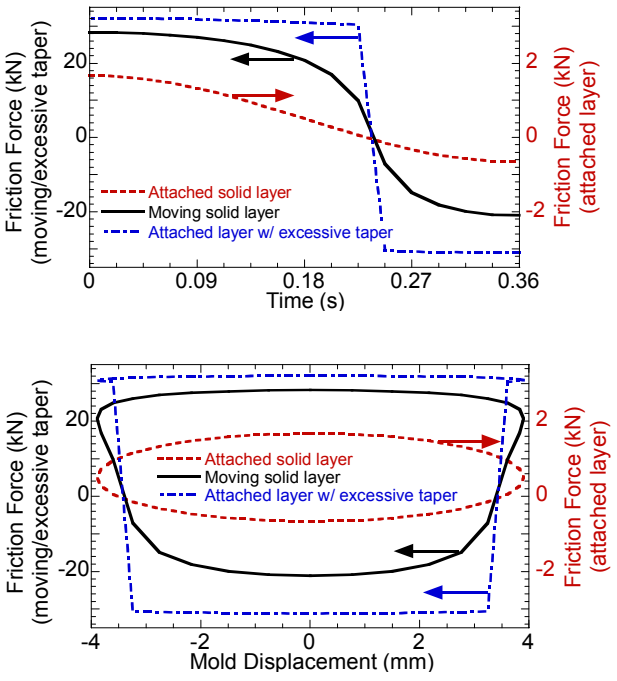

Figure 11 -Friction force over oscillation cycle (Slag A)

high friction forces. Furthermore, they are predicted to change abruptly from tension to compression during the negative strip time. Thirdly, excessive mold taper can squeeze the flux between the shell and the mold, generating even higher friction forces. The predicted mold displacement versus time curves are consistent with measurements. The average total friction force has a minimum at intermediate casting speed, which can be explained by the model in terms of the lubrication consumption, and increasing mold taper problems at higher speed [8].

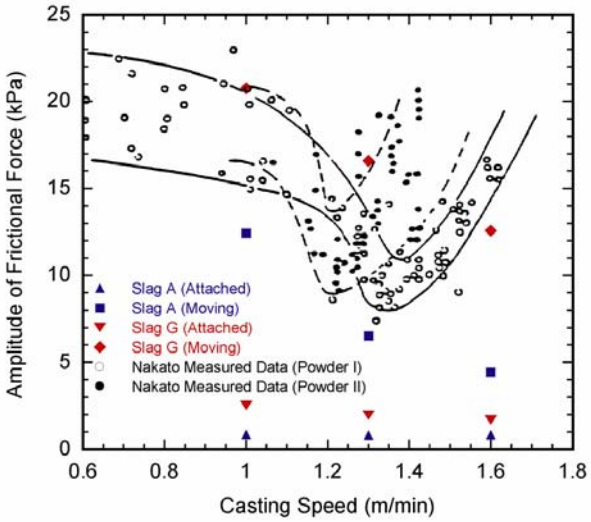

Figure 12 -Effect of casting speed on friction force: measurement and prediction

Stress Modeling of the Solidifying Steel Shell

A coupled finite-element model, CON2D, has been developed to simulate temperature, stress, and shape development during the continuous casting of steel, both in and below the mold [10]. The model simulates a transverse section of the strand in generalized plane strain as it moves down at the casting speed (Figure 13). It includes the effects of heat conduction, solidification, non-uniform superheat dissipation due to turbulent fluid flow, mutual dependence of the heat transfer and shrinkage on the size of the interfacial gap, taper and thermal distortion of the mold. The stress model features an elastic-viscoplastic creep constitutive equation that accounts for the different responses of the liquid, semi-solid, delta-ferrite, and austenite phases. Functions depending on temperature and composition are employed for properties such as thermal linear expansion. A contact algorithm is used to prevent penetration of the shell into the mold wall due to the internal liquid pressure. An efficient two-step algorithm is used to integrate these highly non-linear equations. The model was validated with an analytical solution of temperature and stress in a solidifying slab.

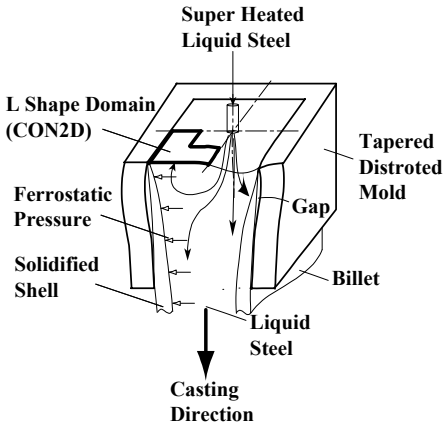

Figure 13. Schematic of billet casting

The model is next validated by applying it to simulate continuous casting of a 120mm square billet [10]. Heat flux across the interface depends on the size of the shrinkage gap, the conductivity of the gap vapor, and the strand roughness. Total heat removal was calibrated to match the measured heatup of the cooling water, as with the CON1D model. Figure 14 shows that the predictions match with thermocouple measurements of mold wall temperature [11]. Figure 15 shows that the model is able to predict shell thickness, including thinning of the corner [11].

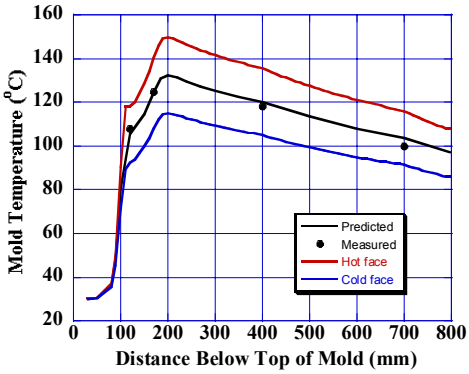

Figure 14 Computed and measured mold temperatures

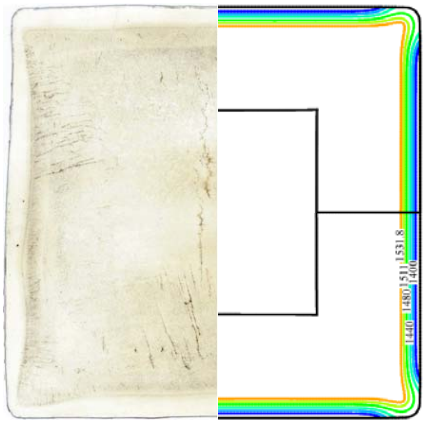

Figure 15: Temperature contours at 285mm below meniscus compared with corresponding sulfur print from plant trial

Optimization of mold taper design

One application of the thermal stress model is to optimize mold taper design, especially of the narrow face [12]. Ideal mold taper is affected by thermal shrinkage of the shell, grade-dependent creep strain, and mold distortion. The heat flux profiles for different steel grades and mold fluxes are shown in Figure 16. Peritectic steels have lower heat flux, owing to their deeper oscillation marks, and high-solidification mold fluxes usually used for these grades. As shown in Figure 17, this causes them to have less shrinkage and less taper, in spite of the phase transformation contraction from delta-ferrite to austenite experienced by these steels.

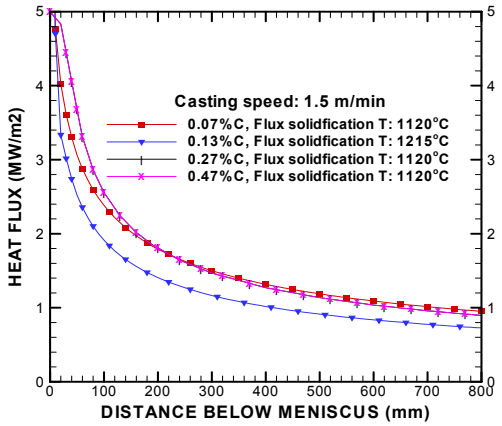

Figure 16: Heat flux profiles for different steel grades (1.5m/min)

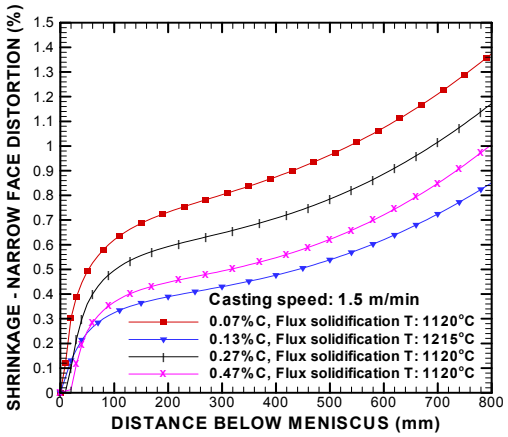

Figure 17: Ideal taper for different steel grades (1.5m/min)

Maximum casting speed to avoid hot-tear cracks

Another application of the stress model is predicting the maximum casting speed to achieve quality steel at maximum productivity [13]. Casting speed can be limited by factors ranging from excessive level fluctuations, mold friction, insufficient metallurgical length, excessive bulging, reheating in the spray zones and many other problems. One of these is the avoidance of longitudinal cracks, such as the one pictured in Figure 19. Hot-tear cracks are predicted to form when the "damage strain" (tensile strain accumulated at the solidification front within

the temperature range between 90 – 99% solid) exceeds a critical value, which depends on steel grade (temperature range across the mushy zone) and strain rate.

With increasing casting speed, the shell thickness at mold exit decreases, and the internal ferrostatic pressure causes bulging. As shown in Figure 18, this causes rotation of the shell near the corner, which generates high strains at the solidification front. The highest damage strains arise at the subsurface off-corner location where the longitudinal cracks are ultimately observed (Figure 19). Casting speed was increased until the maximum damage strain reached the critical value for hot-tear cracks. Results for the critical maximum casting speed are presented in Figure 20 as a function of mold length and section size. Simulations were performed assuming ideal mold taper and uniform temperature below mold (ideal spray cooling). Longer molds allow a thicker shell to form, thus increasing the allowable maximum casting speed. Similarly, smaller section sizes experience much less bulging, so can be cast at higher speed. The quantitative ability of the model is demonstrated by comparison with plant measurements. An implication of the model results is that higher casting speed is possible with carefully aligned foot rolls, and by avoiding mold wear.

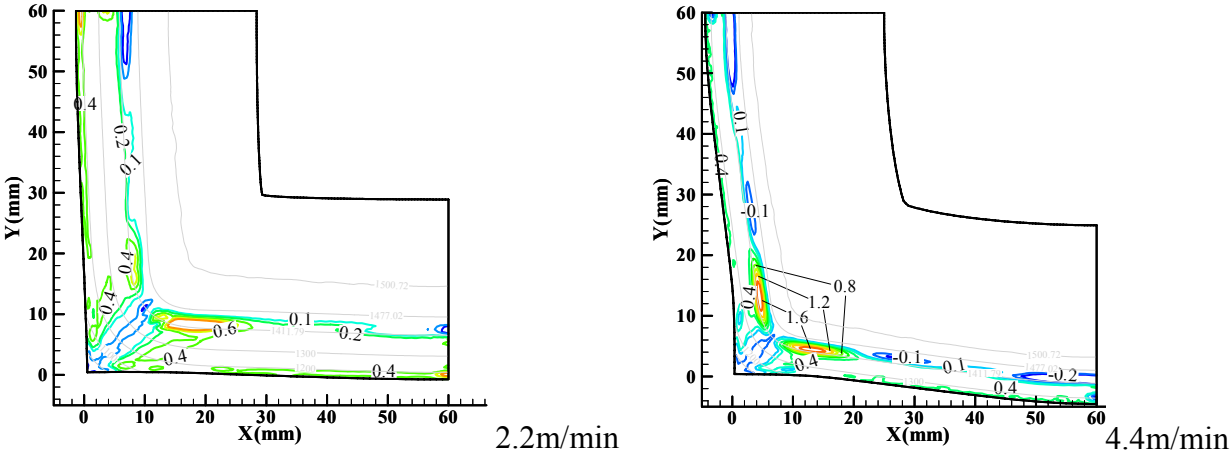

Figure18: Damage Strain Contours at 100 mm below Mold Exit

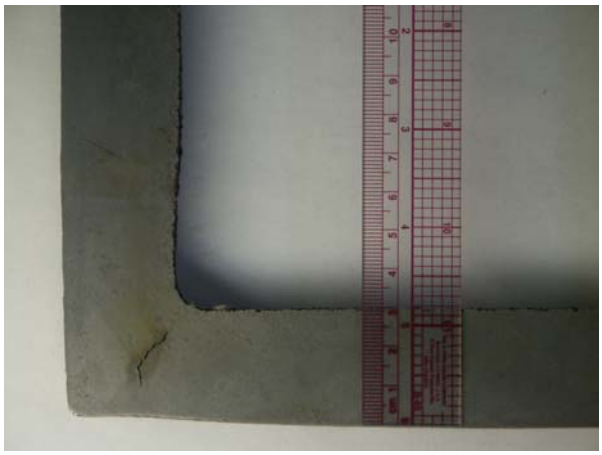

Figure 19: Con-cast billet after breakout showing off-corner sub-surface crack

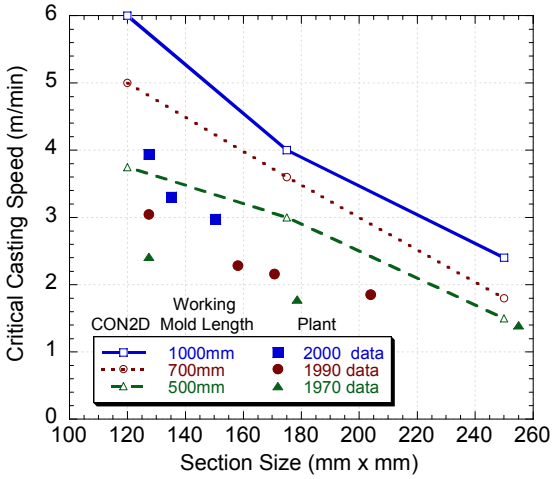

Figure 20: Critical speeds based on off-corner longitudinal crack criterion

Conclusions

This paper has shown how the capability of computational models of continuous casting is growing to generate quantitative understanding of phenomena ranging from fluid flow,

solidification, and stress analysis. These models can generate important practical knowledge, if they include the important phenomena, are subjected to rigorous validation, and then are used in parametric studies of controllable process parameters. This knowledge can be used in many ways, such as designing nozzle and mold shapes, interpreting sensor signals such as mold friction, and putting limits on casting speed to avoid defects. In addition, faster online models can control the liquid steel and cooling water flows, casting speed and other parameters. Improvements to real commercial processes, such as continuous casting must be cost efficient, owing to economic pressure from the general oversupply of primary metals in the world. Thus, future advances require a multifaceted approach, combining plant experiments, lab experiments, and computational models with validation. In particular, future technology advances likely will rely on even better models and control systems.

Acknowledgements

The author thanks the National Science Foundation (Grant DMI-01-15486) and the member companies of the Continuous Casting Consortium at the University of Illinois at Urbana-Champaign (UIUC) for support of this research. Special thanks are due to graduate students who worked on these projects, including Quan Yuan, Ya Meng, and Chunsheng Li, and to the National Center for Supercomputing Applications (NCSA) at UIUC for computer facilities.

References

1. B.G. Thomas, Q. Yuan, L. Zhang, B. Zhao, S.P. Vanka, "Flow Dynamics and Inclusion Transport in Continuous Casting of Steel," in 2004 NSF Design, Service, and Manufacturing Grantees and Research Conf. Proceedings, Southern Methodist Univ, Dallas, TX, (Dallas, TX), 2004, 41p.
2. B.G. Thomas, Q. Yuan, S. Sivaramakrishnan, T. Shi, S.P. Vanka, M.B. Assar, "Comparison of Four Methods to Evaluate Fluid Velocities in CC," ISIJ Internat., Vol. 41 (10), 2001, 1266-1276.
3. Q. Yuan, B.G. Thomas & S.P. Vanka, "Study of Transient Flow and Particle Transport during Continuous Casting of Steel Slabs, I. Fluid Flow," Metall. & Mat. Trans. B, submitted Aug, 2003.
4. Q. Yuan, B.G. Thomas and S.P. Vanka, "Turbulent Flow and Particle Motion in Continuous Slab-Casting Molds," in ISSTech 2003 Process Technology Proceedings, Vol. 86, ISS, Warrendale, PA, (Indianapolis, IN, Apr 27-30, 2003), 2003, 913-927.
5. R.J. O'Malley, personal communication, Middletown, OH, 2003.
6. Q. Yuan, B.G. Thomas & S.P. Vanka, "Study of Transient Flow and Particle Transport during Con. Casting of Steel Slabs, II. Particle Transport," Metal. Mat. Trans. B, accepted Oct, 2003.
7. Y. Meng and B.G. Thomas, "Heat Transfer and Solidification Model of Continuous Slab Casting: CON1D," Metal. & Material Trans., Vol. 34B (5), 2003, 685-705.
8. Y. Meng and B.G. Thomas, "Interfacial Friction-Related Phenomena in Continuous Casting with Mold Slags," in ISSTech 2003 Steelmaking Conf. Proc., Vol. 86, ISS, Warrendale, PA, (Indianapolis, IN, Apr. 27-30, 2003), 2003, 589-606.
9. Y. Kashiwaya, C. Cicutti and A.W. Cramb, "Crystallization Behavior of Mold Slags," in Steelmaking Conf. Proc., Vol. 81, Iron and Steel Soc, Warrendale, PA, 1998, 185-191.
10. C. Li and B.G. Thomas, "Thermo-Mechanical Finite-Element Model of Shell Behavior in Continuous Casting of Steel," Metall. & Materials Trans. B, submitted August, 2003.
11. J.-k. Park, B.G. Thomas and I.V. Samarasekera, "Analysis of Thermo-Mechanical Behavior in Billet Casting with Different Mold Corner Radii," Ironmak. Steelmaking, 29 (5), 2002, 359-375.
12. B.G. Thomas and C. Ojeda, "Ideal Taper Prediction for Slab Casting," in ISSTech 2003 - Manfred Wolf Memorial Symposium Proceedings, Vol. 86, ISS, Warrendale, PA, (Indianapolis, IN, Apr. 27-30, 2003), 2003, 295-308.
13. C. Li and B.G. Thomas, "Maximum Casting Speed for Continuous Cast Steel Billets Based on Sub-Mold Bulging Computation," in Steelmaking Conf. Proc., Vol. 85, ISS, Warrendale, PA, (Nashville, TN, March 10-13, 2002), 2002, 109-130.